ADVANCED FUNCTIONAL MATERIALS
www.afm-journal.de

Nanoscale Ferroelectricity in Crystalline γ-Glycine

*Alejandro Heredia, Vincent Meunier, Igor K. Bdikin, José Gracio, Nina Balke, Stephen Jesse, Alexander Tselev, Pratul K. Agarwal, Bobby G. Sumpter, Sergei V. Kalinin, and Andrei L. Kholkin**

Ferroelectrics are multifunctional materials that reversibly change their polarization under an electric field. Recently, the search for new ferroelectrics has focused on organic and bio-organic materials, where polarization switching is used to record/retrieve information in the form of ferroelectric domains. This progress has opened a new avenue for data storage, molecular recognition, and new self-assembly routes. Crystalline glycine is the simplest amino acid and is widely used by living organisms to build proteins. Here, it is reported for the first time that γ-glycine, which has been known to be piezoelectric since 1954, is also a *ferroelectric*, as evidenced by local electromechanical measurements and by the existence of as-grown and switchable ferroelectric domains in microcrystals grown from the solution. The experimental results are rationalized by molecular simulations that establish that the polarization vector in γ-glycine can be switched on the nanoscale level, opening a pathway to novel classes of bioelectronic logic and memory devices.

1. Introduction

One of the key aspects of biological systems is the intricate relationship between the chemical and electrical functionality, ranging from piezoelectricity in amino-acid derivatives and calcified tissues[1] to the complicated dynamics of the ionic channels and flexoelectricity in cellular membranes.[2] Traditionally, it was believed that the polarization or its electromechanical derivative (e.g., piezoelectricity) in biological systems are defined unambiguously by the structure, and cannot be tuned by external electric fields. In other words, many biomaterials possess piezoelectricity, but ferroelectricity is rather rare. Somewhat contrary to this assumption, many of the early ferroelectrics are in fact partly organic. Rochelle salt is such an example, as it consists of tartrate groups.[3] Another well-known material, triglycine sulfate ($(NH_2CH_2COOH)_3 \cdot H_2SO_4$) (TGS) is probably the most studied.[4] More recently, several crystalline organic materials have been identified as ferroelectrics, but their properties are too mediocre to be used in practical applications.[5] Very recently, a strong ferroelectricity was obtained in croconic acid crystals, showing a spontaneous polarization close to that of barium titanate (≈20 μC cm^{-2}) at room temperature.[6] This prompted a new wave of interest in these low-molecular-weight organic materials. However, despite these advances, a pronounced ferroelectricity in biological and bio-organic materials has so far remained elusive.

Here, we report, for the first time, robust and persistent nanoscale ferroelectricity in the smallest amino acid, glycine, in the piezoelectric γ phase, and demonstrate that ferroelectric behavior can, in principle, persist at a single-molecular level. Glycine ($NH_3^+CH_2COO^-$) has been one of the most studied crystalline amino acids since its discovery over 200 years ago. Its most common polymorph, α form, was identified first by Albrecht and Corey in 1939.[7] An unstable β form was described by Fischer as early as 1900.[8] A third form that exists in ambient conditions, γ-glycine, was discovered by Iitaka in 1954.[9] Glycine is a common material in multiple areas of biology and organic chemistry. The principal function of glycine is to serve as a building block for proteins and as an inhibitory transmitter in the central nervous system.[10] The observed ferroelectric behavior adds a new important functionality to this well-known biomaterial.

2. Results and Discussion

α-glycine is built from dipolar zwitterionic glycine molecules arranged into centrosymmetric cyclic dimers,[11] while in its γ polymorph, the polar molecules are packed into parallel helicoidal chains in head-to-tail arrangements.[12] Therefore, γ-glycine should possess both piezoelectricity and pyroelectricity. While it is well established that γ-glycine is a strong, uniaxial

Dr. A. Heredia, Dr. A. L. Kholkin
Department of Ceramics and Glass Engineering & CICECO
University of Aveiro, 3810-193 Aveiro, Portugal
E-mail: kholkin@ua.pt
Prof. V. Meunier
Physics, Astronomy and Applied Physics Department
Rensselaer Polytechnic Institute
Troy, NY 12180, USA
Dr. I. K. Bdikin, Prof. J. Gracio
Nanotechnology Research Division
Centre for Mechanical Technology & Automation
University of Aveiro
3810-193 Aveiro, Portugal
Dr. N. Balke, Dr. S. Jesse, Dr. A. Tselev, Dr. P. K. Agarwal, Dr. B. G. Sumpter, Dr. S. V. Kalinin
Oak Ridge National Laboratory
Oak Ridge, TN 37830, USA

DOI: 10.1002/adfm.201103011

piezoelectric,[8] pyroelectricity and ferroelectricity in this organic compound have not been reported thus far. In this work, glycine microcrystals were prepared by the slow evaporation of a supersaturated solution at different temperatures,[12,13] and the presence of the γ polymorph was confirmed by Fourier transform IR (FTIR) spectroscopy measurements (see Supporting Information). To establish the possible ferroelectric nature of the as-grown polycrystalline and single-crystalline glycine, we used piezoresponse force microscopy (PFM), a powerful tool for studying piezoelectric and ferroelectric phenomena at the micro- and nanometer-scale levels.[14] In this method, a sharp conductive tip in contact with the surface is periodically biased, and bias-induced surface displacements are translated into the mechanical motion of the tip (see schematic in **Figure 1** a,b). Both out-of-plane (OOP) and in-plane (IP) displacements have been monitored, uncovering apparent nanoscale piezoelectric and ferroelectric properties of glycine crystals. Representative PFM images of a polycrystalline glycine sample grown on the $Pt/SiO_2/Si$ substrates are shown in Figure 1c–e. These images reveal a complex PFM signal, where the α (centrosymmetric, no piezoresponse) and γ (piezoelectric, distinct OOP and IP contrasts) phases coexist, as can be judged from their respective PFM images. We did not find any preferred orientation of the polarization direction in the γ phase. This suggests heterogeneous nucleation and random growth of the glycine microcrystals. For the OOP component (Figure 1d), the PFM contrast is proportional to the effective (longitudinal) piezoelectric coefficient, d_{33}, of γ-glycine. The dark and bright colours correspond to the polarization directed toward the substrate and toward the surface, respectively. This polarization component apparently varies in direction and magnitude (value of the d_{33} coefficient) and depends on the orientation of the as-grown microcrystals. The IP piezoresponse image (Figure 1e) is complementary to the OOP image, reflecting an effective (shear) piezoelectric coefficient, d_{15}, that is proportional to the in-plane component of the polarization. The effective longitudinal piezocoefficients, measured by PFM, are about 10 pm V^{-1} (based on a calibration procedure performed with $LiNbO_3$ single crystals[15]).

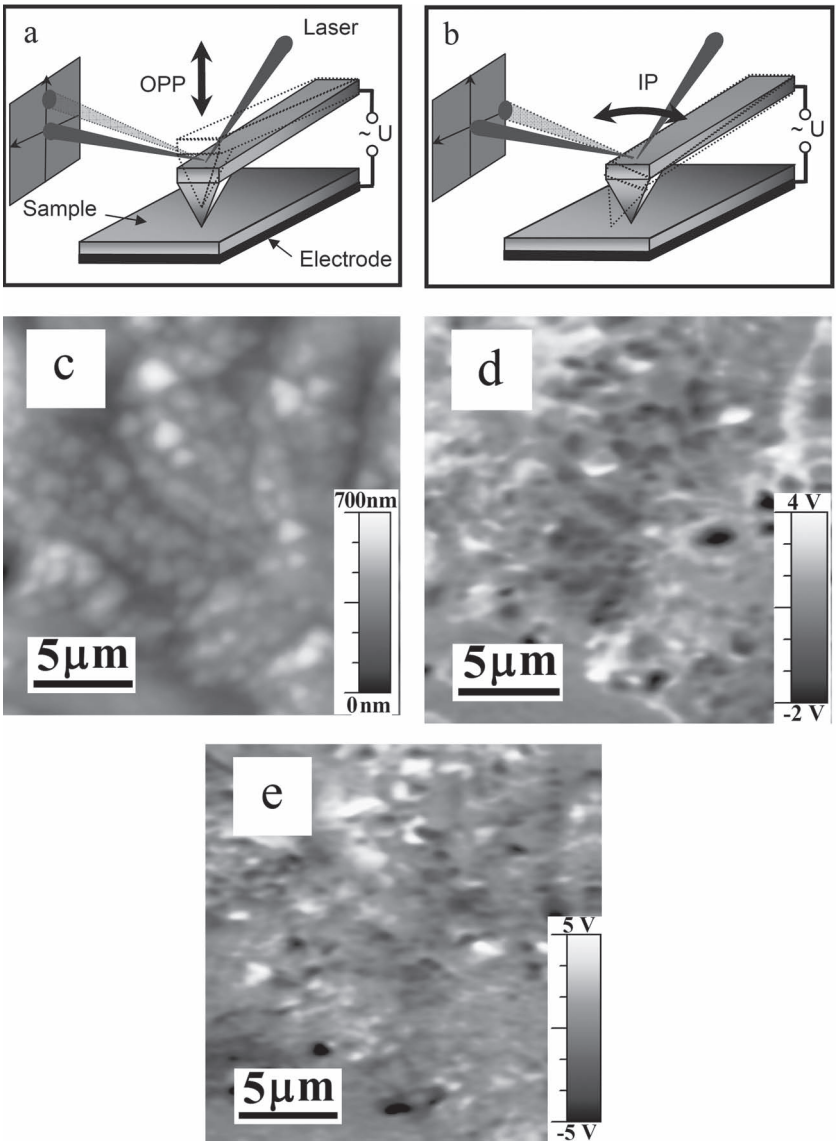

Figure 1. a,b) Schematics of the acquisition of PFM images in out-of-plane (OOP) (a) and in-plane (IP) (b) configurations. c–e) Topography (c), OOP (d) and IP (e) signals for the glycine sample grown from solution on a $Pt/SiO_2/Si$ substrate. The images were taken simultaneously on the same area. The black and white areas are attributed to γ-glycine.

We observed a pure γ phase in the crystals that could be grown separately as microislands, as evidenced by our PFM experiments. This result is consistent with recent work by Lee et al.,[16] where pure γ-glycine was grown from small droplets confined to metallic gold islands. A representative topography image of one of our microcrystals is shown in **Figure 2** a. PFM contrast can be observed over the entire surface of the as-grown microcrystal (Figure 2 b). This suggests that only the γ polymorph was formed under these conditions. As is clearly seen from Figure 2 b, areas with different polarization directions (ferroelectric 180° domains with polarization vectors oriented normal to the substrate) were spontaneously formed in the γ-glycine. This was proven by the absence of the IP (lateral) response (Figure 2 c), irrespective of the scanning direction. Relatively sharp boundaries separating the antiparallel polarization domains were found with the wedge-like domain morphology that is typical for ferroelectrics. Planar domain walls were primarily observed, as is common for ferroelectrics without defects.[2] It should be stressed that the as-grown crystals were nonpolar on the macroscopic scale, and the small size of the ferroelectric domains in the crystals explains the inability to detect the ferroelectric properties of γ-glycine with low-resolution optical methods in earlier studies.[17]

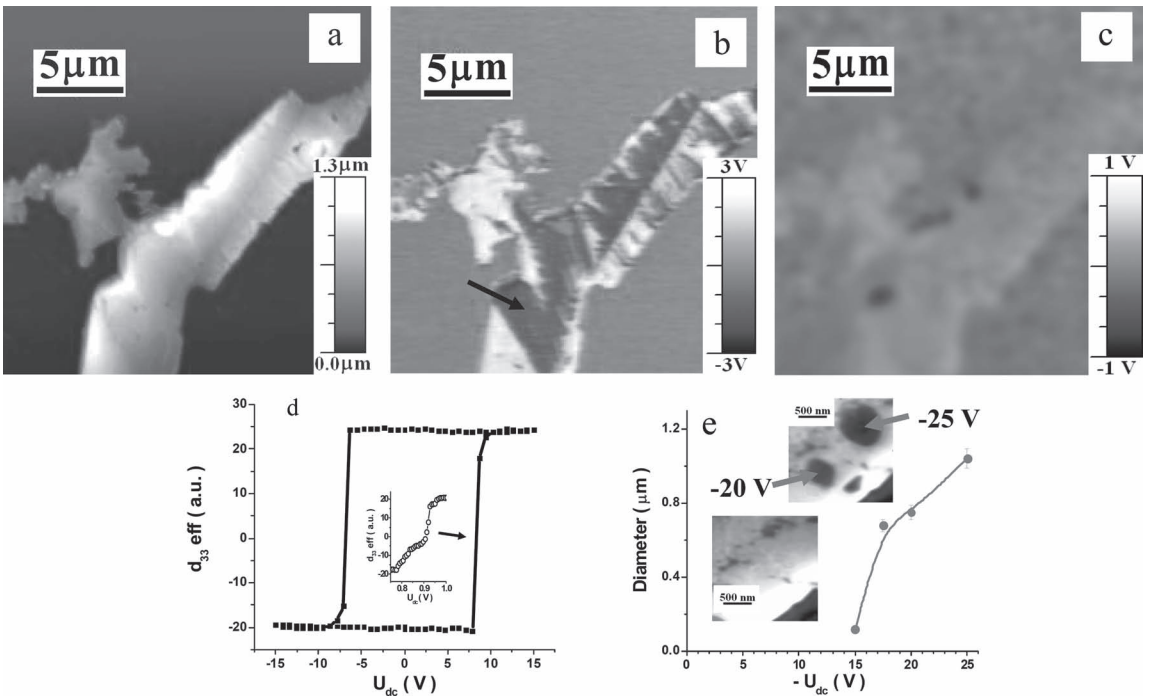

Figure 2. a–d) Topography (a), OOP (b), and IP (c) PFM images, and the representative piezoresponse hysteresis loop (d) obtained in the γ-glycine microcrystal. The arrow in Figure 2b shows the point where the local hysteresis was acquired. e)The ferroelectric domain diameter *D* as a function of applied voltage *V* at a constant writing time $\tau = 0.1$ s. The insets in Figure2e show artificial domains written under –25 and –20 V, applied between the PFM tip and the counter electrode.

Using PFM switching spectroscopy,[18] we further confirmed the ferroelectricity in glycine, and proved its polarization switchability under an external electric field. In this experiment, a dc-voltage bias applied to the PFM tip at a chosen location was swept in a cyclic manner to obtain piezoresponse hysteresis loops (Figure 2d). We could also visualize electrically written, circular ferroelectric domains (inset to Figure 2e) and establish a relation between their diameter (Figure 2e) and the applied bias, as is common in studies of inorganic ferroelectrics (as has been reviewed recently by Kalinin et al.[19]). In these measurements, the PFM tip was fixed at a predefined location on the sample surface and strong bias pulses (up to 25 V) were applied between the tip and the counter electrode. The subsequent imaging allowed detection of bias-induced changes in the domain structure, *unequivocally* proving their ferroelectric nature. Note that the evolution of the domain size with bias indicates the presence of a well-defined threshold for ferroelectric domain nucleation (approximately –15 V for a pulse duration of 0.1 s) and a gradual increase of the domain diameter with bias above this threshold, similar to PFM switching experiments in classical ferroelectric materials such as $LiNbO_3$[20] and $BaTiO_3$.[21] In this way, due to polarization reversal, polarization dots less than 100 nm in diameter could be formed in predefined locations on the surface of the γ-glycine. This behavior reflects the growth of reversed domains under increasing voltage due to increasing electric field at the domain boundary and can be used for the development of dense polarization-based memory.[22] It is worth noting that the observed, well-defined piezoresponse hysteresis loop (shown in Figure 2d) is a clear signature of polarization switching on the local scale. It provides many important parameters of the ferroelectric material, such as values of the piezoelectric coefficient (proportional to the polarization), nucleation bias (the threshold for the piezocontrast increase), imprint (the shift of the loop along the bias axis), and work of switching (directly proportional to the area encompassed by the loop).[23] It should be also mentioned that the hysteresis loops were quite symmetric, the nucleation threshold being very sharp, which indicates that the nascent reverse polarization domain grew rapidly under increasing bias, without any evidence of the domain pinning characteristic for ferroelectrics with defects.[24] This feature could be extremely useful for possible applications in information storage devices, as short voltage pulses applied to the tip can be used for the creation of stable information bits. The spatial variability of the switching behavior in γ-glycine was explored by switching spectroscopy combined with the band excitation (BE) method,[25] in which hysteresis loops are acquired over a densely spaced square grid of points on the sample surface. **Figure 3**a,b shows a region of an as-grown microcrystal containing two stripe domains. After switching on a 20 × 20 grid with ±25 V, the polarization of the whole area switched (Figure 3c), which confirms that the domains in γ-glycine could be fully reversed over a large area. The variability of the switching behavior was visualized as 2D maps of switching parameters extracted from the hysteresis loops. As an example, a map of the positive coercive voltage is shown in Figure 3d. The image presents a clear correlation of the positive coercive voltage with the as-grown domain structure (Figure 3b). The switching behavior was nearly

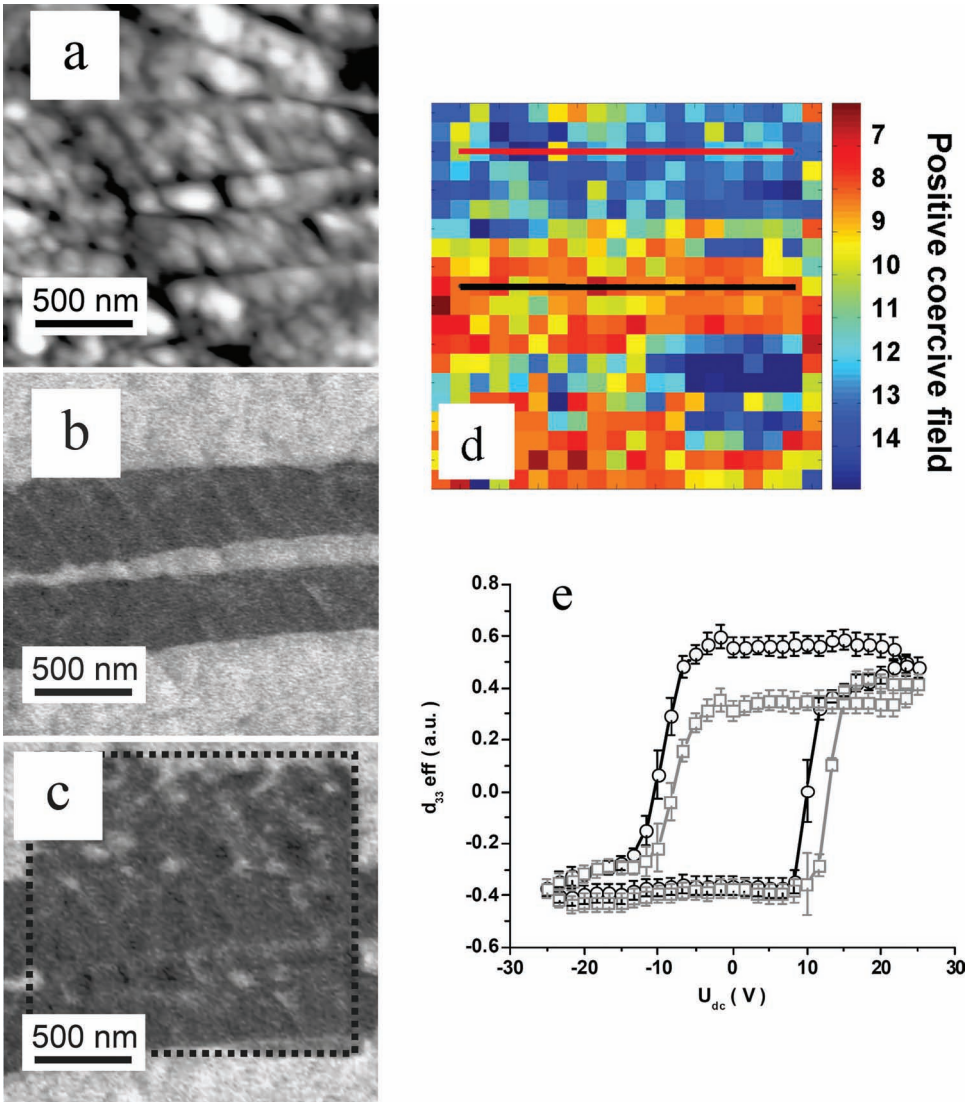

Figure 3. Spatially resolved ferroelectric switching in γ-glycine. a–c) Topography (a), and PFM in plane before (b) and after (c) switching on a 20 × 20 grid in the indicated area. d) A map of the positive coercive field in the switched area. e) Hysteresis loops extracted from the lines shown in Figure 3d.

uniform within domains having bright and dark PFM contrast, and the ferroelectric switching in the dark domains required a lower voltage. Figure 3e displays averaged loops extracted from the two different areas indicated in Figure 3d. The hysteresis loops extracted from the dark domains are more symmetric (i.e., they exhibit a smaller shift along the voltage axis). This indicates a lower internal bias field inherent to organic ferroelectrics with permanent dipoles.[3]

Further evidence of the ferroelectric phase transition in γ-glycine was obtained from measurements of the dielectric constant in pressed microcrystals (**Figure 4**). The dielectric constant, ε, demonstrates a distinct maximum at a temperature of 210 °C under an ac electric field with a frequency of 1 MHz, which is characteristic of a phase transition into a paraelectric state. Fitting with the classical Curie–Weiss law, $1/\varepsilon = -(T - T_{Cb})/C_{Wb}$, provided important parameters: the Curie–Weiss temperature, $T_{Cb} = 300 \pm 1$ °C, and a value of the Curie–Weiss constant, $C_{Wb} \approx 2000 \pm 10$ °C (see inset in Figure 4a). Above the phase transition, the dielectric constant obeys the Curie–Weiss law, $1/\varepsilon = (T - T_{Ca})/C_{Wa}$, as well, but the data were not reproducible, perhaps due to the strong degradation of the samples with increasing temperature (the compound decomposed at $T \approx 233$ °C). The large difference between the transition temperature T_c (the temperature of the dielectric maximum in Figure 4a) and the Curie–Weiss temperature indicates a first-order phase transition, and the value of the Curie–Weiss constant is characteristic of the order-disorder phase transition.[3] High dielectric loss at low frequency (Figure 4b) obscured any ferroelectric-type anomalies still seen at higher frequencies.

To elucidate the origins of the ferroelectricity in γ-glycine, the crystal structure and the polarization dynamics in an external electric field were studied using density functional theory (DFT) and molecular-dynamics (MD) simulations. The crystal structure of the γ phase (symmetry group $P3_2$) was determined in the

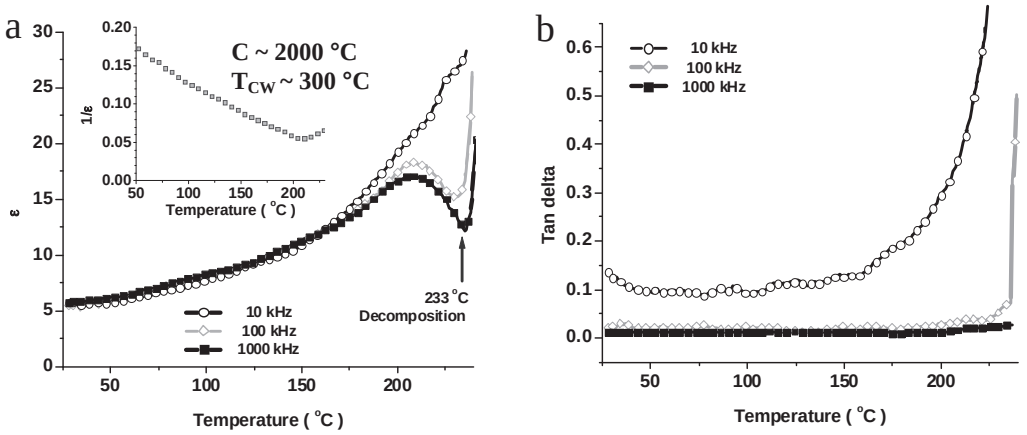

Figure 4. Dielectric constant (a) and loss tangent (b) vs. temperature dependences in pressed glycine sample at different frequencies.

calculations as $a = b = 7.008$ Å, $c = 5.460$ Å, $\alpha = 120°$, compared with the experimental data for the lattice given by: $a = b = 7.037$ Å, $c = 5.483$ Å, $\alpha = 120°$.[26] The crystal structure was obtained using a primitive unit cell and a reciprocal-space sampling including 48 *k*-points). Setting the energy reference as the total energy of an isolated zwitterion (i.e., $F_{isolated} = 0.0$ eV), the crystal energy was found to be $F = -1.91$ eV per molecule (i.e., 1.91 eV is the crystal energy compared with individual molecular constituents). The non-zwitterionic isomer, NH_2CH_2COOH, is not stable at a pH close to 7.0 in water or as a solid, but is stable in the gas phase with $F = -1.11$ eV per molecule. This also indicates that, in the crystalline form, the zwitterionic form is preferred by 0.8 eV per molecule. We also computed the energy corresponding to a crystal of $2 \times 2 \times 2$ cells crystal where a single molecule was rotated by 180° around an axis perpendicular to the *c*-axis. We found that the energy required for this rotation was $F = -1.53$ eV per molecule. In other words, despite the large energy penalty, this crystal was still stable, compared with the gas phase.

To study the polarization switching dynamics, we employed classical MD simulations with parameters fitted based on the above quantum calculations.[27] Such a force-field allows a reasonable description of H bonds and non-bonding interactions.[28] In our calculation, we used a simulation box with 648 zwitterion molecules and imposed periodic boundary conditions corresponding to the γ polymorph. In the simulations, a central, essentially cylindrical, region was allowed to move freely, while the molecules in the surrounding area were fixed to their initial positions, thereby mimicking the finite-size area affected by an applied external electric field. MD simulations were performed for a series of electric fields ranging from 0 to 13 V nm^{-1} and the number of switched molecules was computed as a function of the electric field strength (**Figure 5**).

We observed a well-defined transition at ≈4 V nm^{-1}, corresponding to the switching of the majority of the glycine molecules. The switching of the cylindrical domain was complete at ≈8 V nm^{-1}. The incomplete switching points correspond to a situation where some molecules at the boundary of the artificial domain do not switch, but rather align their dipole moments with those of the molecules outside the switchable domain. We could further analyze the data using the values of crystal-formation energy (CFE = –1.91 eV per molecule) and single-molecule rotation energy (SRE = –1.53 eV per molecule) discussed above: since each molecule established strong interactions with 3 neighbors, we could roughly attribute one third of the formation energy (CFE) to each interaction between two molecules in the crystal. Therefore, the minimum energy to break one interaction is ≈CFE/3, to break 2 interactions is ≈2CFE/3 and to break all three interactions is CFE. The first transition should occur for a field slightly larger than that corresponding to CFE/3 because of environmental effects. Likewise, the transition toward 100% should happen for field amplitudes slightly smaller than CFE. This analysis, based on the DFT results, explains the features observed in Figure 5a, obtained from classical MD simulations, remarkably well.

The results of the MD simulations are well supported by the available experimental data (Figure 2). We observed that the piezoresponse signal (roughly proportional to the number of switched glycine molecules) shows switching at a tip voltage of about 8 V. This roughly corresponds to a maximum electric field of the order of 1 V nm^{-1} at the tip apex, with an effective diameter of 8–10 nm (the maximum electric field is determined by the tip diameter[19]). The saturation of the piezosignal at higher voltages is a clear signature of the complete reversal of the ferroelectric domain with a size significantly exceeding the tip diameter.

Remarkably, the origin of ferroelectricity in γ-glycine microcrystals is profoundly different from that in the classical ferroelectric, triglycine sulphate (TGS).[29] TGS is one of the few ferroelectrics with a pure second-order phase transition (which has been the object of fundamental studies for over 50 years, since its discovery by Matthias et al.[29]) and is one of the best materials for pyroelectric sensors. The polar glycine groups in TGS are packed in antiparallel, anti-ferroelectric order and are oriented approximately perpendicular to the polarization axis. The ferroelectric instability in TGS comes from proton ordering in the double-well potential of a hydrogen bond between two adjacent groups positioned head-to-tail – glycine II and glycine III – in the TGS unit cell. Another mechanism is the repositioning of nitrogen in isolated glycine-I groups, which can be visualized as a result of glycine-group rotation approximately along the C–C bond (along

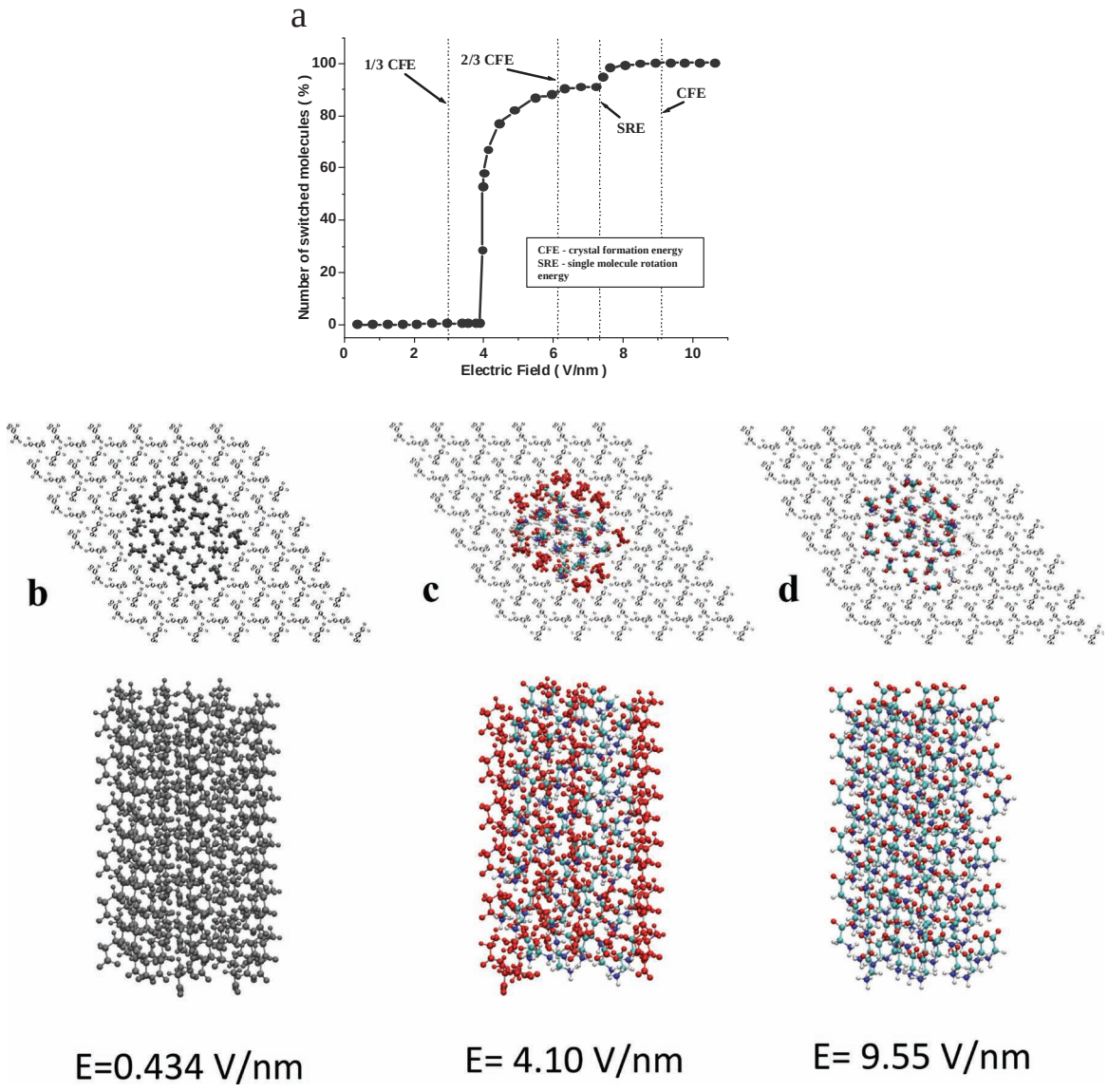

Figure 5. a) The number of glycine molecules switched due to the application of an external electric field. b–d) Steady-state configurations (side- and top- views) of the glycine crystal after electric fields with amplitudes of 0.434, 4.10 and 9.55 V nm^{-1} are applied for a time long enough for full equilibrium to be reached. The molecules that were not allowed to switch are shown in grey in the snapshots.

the molecule), not perpendicular to it, in contrast to γ-glycine. Consequently, while both compounds have ferroelectric-paraelectric phase transitions of the same order-disorder type, the thermodynamical parameters of the transitions in γ-glycine and TGS are dramatically different. γ-glycine demonstrates a first-order phase transition, as opposed to the second-order in TGS, with a significantly higher phase transition temperature (T_C = 210 °C in γ-glycine, as opposed to T_C = 49 °C in TGS).

3. Conclusions

The key implication of the experimental and theoretical analysis above is that ferroelectricity in γ-glycine microcrystals can arise due to flips of the polar glycine molecules in the molecular chains, and, as a result, well-aligned, regular polarization domains are formed due to appearance of the spontaneously polarized state. On the other hand, modelling demonstrates that, in principle, one or a few glycine molecules can be switched if a sufficiently high electric field is applied via the tip. The small size of the glycine molecules may lead to the realization of extremely small polarization bits potentially being applicable, e.g., for ultradense information storage, which is intrinsically impossible with common ferroelectrics.

Beyond information storage, these studies open up a set of interesting possibilities regarding the role of glycine piezoelectricity and ferroelectricity in the genesis of life (e.g., protein formation), as well as emerging properties in peptides from the biophysical point of view. These possibilities stem from their ability to self-assemble locally in a nearly crystalline fashion,

giving rise to ferroelectric activity at the nanoscale. It is well known that a strong electric field can significantly promote biochemical reactions and thus cause simultaneous polarization switching, thereby modifying the catalytical activity of glycine. Furthermore, these properties open up an intriguing set of applications for nanoscale, organic, ferroelectric-based memory (e.g., using the synergy with DNA-based conductors). These are challenges to address in future interdisciplinary research, wherein biochemical and physical polarization phenomena are combined and interrelated on the nanoscale.

4. Experimental Section

Materials: In ambient conditions, γ-glycine possesses the lowest free energy and thus is thermodynamically stable. However, γ-glycine may easily transform into the α form at high temperatures, as these forms are enantiotropically interrelated. Typically, α-glycine is produced from water solutions (at the isoelectric point) while the γ form requires either acidic or basic solutions. β-glycine is metastable and can be only stabilized in specific conditions (e.g., in nanoscale geometries). It has been known for a long time that α-glycine is built from centrosymmetric zwitterionic dimers (space group $P2_1/n$)[30] and γ form consists of polar chains (non-centrosymmetric space group $P3_2$).

We prepared the glycine samples by the method of slow evaporation of a supersaturated solution at different temperatures. The X-ray powder diffraction analysis was performed using powdered samples prepared by this method at room temperature.[31] The obtained X-ray diffraction spectra (Figure S1, Supporting Information) substantiated the presence of glycine as both α and γ polymorphs in a ratio of about 60/40. The positions of the peaks were found to be in good agreement with the data available in JCPDS files. No additional phases were found. Attenuated-total-reflection FTIR (ATR-FTIR) spectroscopy was also used to confirm the existence of the pure glycine in the α and γ forms (see Figure S2). The precipitation of the crystals after its dissolution in water transformed nearly all of the solid from α to γ polymorph, although both phases coexisted, as could be seen from the identified peaks.

Dielectric measurements: For the dielectric measurements, the glycine powder was cold-pressed into cylindrical pellets 10 mm in diameter and 0.4 mm thick using a hydraulic press with a pressure of 100 MPa. Silver electrodes were then deposited by sputtering. The dielectric constant was measured with an HP 4284A Precision LCR meter as a function of temperature, using a home-made furnace.

Piezoresponse Force Microscopy (PFM): The glycine microcrystals were visualized by atomic force microscopy (AFM) and PFM methods. The PFM technique is based on the detection of the mechanical response of the sample to an applied electric voltage due to the converse piezoelectric effect. In this way, both the contact topography and the vertical and lateral piezoresponse signals can be visualized. In our study, a commercial atomic force microscope (Ntegra Prima, NT-MDT) with a conductive Si cantilever (Nanosensors, force constant 15 N m^{-1}) was equipped with an external lock-in amplifier (SR830, Stanford Research) and a function generator (FG120, Yokogawa), which were used in order to apply both ac and dc voltages to the microcrystal surface for poling and further piezoresponse image acquisition.[18] To prove the presence of ferroelectric polarization, we performed PFM switching analysis to obtain hysteresis loops and to correlate the growth of the ferroelectric domains under different bias voltages. In switching measurements, the tip was fixed at a predefined location on the sample surface and a strong bias pulse was applied.

Modelling: The dynamics of the glycine crystals were simulated on a time-scale indicated below using classical force-fields. The simulations were performed using NAMD (v2.7b1) based on AMBER (see Case et al.[32]) co-ordinates and topology files. The AMBER molecular-model building tools were used to prepare the topology and coordinates for a monoclinic crystal cell with dimensions of 59.198 × 37.309 × 34.914 Å, containing 648 glycine molecules. AMBER's parm03 force-field was used for the classical potentials (bonded and nonbonded terms) and the charges for the zwitterionic form were derived using the standard AMBER protocol for charge calculations. The cut-offs for the Lennard–Jones and electrostatic interactions were set at 9 Å and the particle mesh Ewald (PME) method was used for long-range electrostatic calculations with a grid space of 1 Å. For each value of the external electric field, the system was first relaxed for 5000 fs (5 ps). The system was thermalized under MD with *NVE*/*NVT* conditions for 40 000 fs (40 ps) at a temperature T = 300 K. The electric field was then applied for 200 000 fs (200 ps) at T = 300 K. Finally, the system was slowly thermally annealed under zero field from T = 300 K to T = 0 K over 160 000 fs (160 ps) each, before a final geometry relaxation of 200 000 fs (200 ps). The DFT calculations were performed with VASP, using PBE for the exchange-correlation functional.[33] A high energy cut-off was employed to determine the geometry and lattice parameters, using Brillouin Zone sampling as explained in the text.

Supporting Information

Supporting Information is available from the Wiley Online Library or from the author.

Acknowledgements

This research was supported in part (S.V.K., N.B., S.J., A.T., and B.G.S.) by the Center for Nanophase Materials Sciences (CNMS), which is sponsored at Oak Ridge National Laboratory by the Scientific User Facilities Division, Office of Basic Energy Sciences, U.S. Department of Energy, and by the CNMS user program (A.L.K.). I.B. gratefully acknowledges his "Ciência 2008" grant from the Portuguese Foundation for Science and Technology (FCT). V.M. was supported in part by New York State under NYSTAR contract C080117. The Marie-Curie ITN project "Nanomotion" (FP7-PEOPLE-2011-ITN-290158) is acknowledged for partial support.

Received: December 13, 2011
Revised: February 13, 2012
Published online: April 18, 2012

[1] E. Fukada, I. Yasuda, *J. Phys. Soc. Jpn.* **1957**, *12*, 1158.
[2] T. Todorov, A. G. Petrov, J. H. Fendler, *Langmuir* **1994**, *10*, 2344.
[3] J. Valasek, *Phys. Rev.* **1921**, *17*, 475.
[4] M. E. Lines, A. M. Glass, *Principles and Applications of Ferroelectrics and Related Materials*, Clarendon Press, Oxford **2001**, Ch. 9.
[5] S. Horiuchi, Y. Tokura, *Nat. Mater.* **2008**, *7*, 357.
[6] S. Horiuchi, Y. Tokunaga, G. Giovannetti, S. Picozzi, H. Itoh, R. Shimano, R. Kumai, Y. Tokura, *Nature* **2010**, *463*, 789.
[7] G. Albrecht, R. B. Corey, *J. Am. Chem. Soc.* **1939**, *61*, 1087.
[8] E. Fischer, E. Fourneau, *Ber. Dtsch. Chem. Ges.* **1901**, *34*, 2868.
[9] Y. Iitaka, *Proc. Jpn. Acad.* **1954**, *30*, 109.
[10] C. U. M. Smith, *Elements of Molecular Neurobiology*, 2 ed., Wiley, Chichester **2002**.
[11] Y. Iitaka, *Acta Crystallogr.* **1961**, *14*, 1.
[12] I. S. Lee, K. T. Kim, A. Y. Lee, A. S. Myerson, *Cryst. Growth Design* **2008**, *8*, 108.
[13] R. E. Marsh, *Acta Crystallogr.* **1958**, *11*, 654.
[14] S. V. Kalinin, N. Setter, A. L. Kholkin, *MRS Bull.* **2009**, *34*, 634.
[15] A. Kholkin, N. Amdursky, I. Bdikin, G. Rosenman, E. Gazit, *ACS Nano* **2010**, *4*, 610.
[16] A. Y. Lee, I. S. Lee, S. S. Dette, J. Boerner, A. S. Myerson, *J. Am. Chem. Soc.* **2005**, *127*, 14982.

[17] K. S. Kunihisa, *Mol. Cryst. Liq. Cryst.* **1975**, *30*, 233.
[18] A. L. Kholkin, S. V. Kalinin, A. Roelofs, A. Gruverman, in *Scanning Probe Microscopy: Electrical and Electromechanical Phenomena at the Nanoscale*, Vol. *I*, (Eds: S. Kalinin, A. Gruverman), Springer, New York **2006**.
[19] S. V. Kalinin, A. N. Morozovska, L. Q. Chen, B. J. Rodriguez, *Rep. Prog. Phys.* **2010**, *73*, 056502.
[20] B. J. Rodriguez, R. J. Nemanich, A. Kingon, A. Gruverman, S. V. Kalinin, K. Terabe, X. Y. Liu, K. Kitamura, *Appl. Phys. Lett.* **2005**, *86*, 012906.
[21] N. Pertsev, A. Petraru, I. Bdikin, D. Kiselev, A. L. Kholkin, *Nanotechnology* **2008**, *19*, 375703.
[22] C. H. Ahn, K. M. Rabe, J.-M. Triscone, *Science* **2004**, *303*, 488.
[23] S. V. Kalinin, A. Gruverman, D. A. Bonnell, *Appl. Phys. Lett.* **2004**, *85*, 795.
[24] S. V. Kalinin, S. Jesse, B. J. Rodriguez, Y. H. Chu, R. Ramesh, E. A. Eliseev, A. N. Morozovska, *Phys. Rev. Lett.* **2008**, *100*, 155703.
[25] S. Jesse, S. V. Kalinin, R. Proksch, A. P. Baddorf, B. J. Rodriguez, *Nanotechnology* **2007**, *18*, 435503.
[26] Z. Latajka, H. Ratalczak, *J. Phys. Chem.* **1979**, *83*, 2785.
[27] C. I. Bayly, P. Cieplak, W. Cornell, P. A. Kollmann, *J. Phys. Chem.* **1993**, *97*, 10269.
[28] C. D. Sherrill, B. G. Sumpter, M. O. Sinnokrot, M. S. Marshall, E. G. Hohenstein, R. C. Walker, I. R. Gould, *J. Comput. Chem.* **2009**, *30*, 2187.
[29] B. T. Matthias, C. E. Miller, J. P. Remeika, *Phys. Rev. B: Condens. Matter* **1956**, *104*, 849.
[30] R. E. Marsh, *Acta Crystallogr.* **1958**, *11*, 654.
[31] I. S. Lee, K. T. Kim, A. Y. Lee, A. S. Myerson, *Cryst. Growth Design* **2008**, *8*, 108.
[32] D. A. Case, T. E. Cheatham, T. Darden, H. Gohlke, R. Luo, K. M. M. A. Onufriev Jr., C. Simmerling, B. Wang, R. J. Woods, *J. Comput.Chem.* **2005**, *26*, 1668.
[33] a) G. Kresse, J. Furthmuller, *Comput. Mater. Sci.* **1996**, *6*, 15; b) G. Kresse, J. Furthmuller, *Phys. Rev. B* **1996**, *54*, 11169.